Preclinical Comparison of Al[18]F- and ^{68}Ga-Labeled Gastrin-Releasing Peptide Receptor Antagonists for PET Imaging of Prostate Cancer

Kristell L.S. Chatalic[1,2], Gerben M. Franssen[3], Wytske M. van Weerden[2], William J. McBride[4], Peter Laverman[3], Erik de Blois[1], Bouchra Hajjaj[5], Luc Brunel[5], David M. Goldenberg[4], Jean-Alain Fehrentz[5], Jean Martinez[5], Otto C. Boerman[3], and Marion de Jong[1]

[1]Department of Nuclear Medicine, Erasmus MC, Rotterdam, The Netherlands; [2]Department of Urology, Erasmus MC, Rotterdam, The Netherlands; [3]Department of Nuclear Medicine, Radboud University Medical Center, Nijmegen, The Netherlands; [4]Immunomedics, Inc., Morris Plains, New Jersey; and [5]Institut des Biomolécules Max Mousseron, UMR 5247, CNRS-UM1-UM2, Montpellier, France

Gastrin-releasing peptide receptor (GRPR) is overexpressed in human prostate cancer and is being used as a target for molecular imaging. In this study, we report on the direct comparison of 3 novel GRPR-targeted radiolabeled tracers: Al[18]F-JMV5132, ^{68}Ga-JMV5132, and ^{68}Ga-JMV4168 (JMV5132 is NODA-MPAA-βAla-βAla-[H-D-Phe-Gln-Trp-Ala-Val-Gly-His-Sta-Leu-NH₂], JMV4168 is DOTA-βAla-βAla-[H-D-Phe-Gln-Trp-Ala-Val-Gly-His-Sta-Leu-NH₂], and NODA-MPAA is 2-[4-(carboxymethyl)-7-{[4-(carboxymethyl) phenyl]methyl}-1,4,7-triazacyclononan-1-yl]acetic acid). **Methods:** The GRPR antagonist JMV594 (H-D-Phe-Gln-Trp-Ala-Val-Gly-His-Sta-Leu-NH₂) was conjugated to NODA-MPAA for labeling with Al[18]F. JMV5132 was radiolabeled with ^{68}Ga and ^{18}F, and JMV4168 was labeled with ^{68}Ga for comparison. The inhibitory concentration of 50% values for binding GRPR of JMV4168, JMV5132, natGa-JMV4168, and natGa-JMV5132 were determined in a competition-binding assay using GRPR-overexpressing PC-3 tumors. The tumor-targeting characteristics of the compounds were assessed in mice bearing subcutaneous PC-3 xenografts. Small-animal PET/CT images were acquired, and tracer biodistribution was determined by ex vivo measurements. **Results:** JMV5132 was labeled with ^{18}F in a novel 1-pot, 1-step procedure within 20 min, without need for further purification and resulting in a specific activity of 35 MBq/nmol. Inhibitory concentration of 50% values (in nM) for GRPR binding of JMV5132, JMV4168, natGa-JMV5132, natGa-JMV4168, and Al[nat]F-JMV5132 were 6.8 (95% confidence intervals [CIs], 4.6–10.0), 13.2 (95% CIs, 5.9–29.3), 3.0 (95% CIs, 1.5–6.0), 3.2 (95% CIs, 1.8–5.9), and 10.0 (95% CIs, 6.3–16.0), respectively. In mice with subcutaneous PC-3 xenografts, all tracers cleared rapidly from the blood, exclusively via the kidneys for ^{68}Ga-JMV4168 and partially hepatobiliary for ^{68}Ga-JMV5132 and Al[18]F-JMV5132. Two hours after injection, the uptake of ^{68}Ga-JMV4168, ^{68}Ga-JMV5132, and Al[18]F-JMV5132 in PC-3 tumors was 5.96 ± 1.39, 5.24 ± 0.29, 5.30 ± 0.98 (percentage injected dose per gram), respectively. GRPR specificity was confirmed by significantly reduced tumor uptake of the 3 tracers after coinjection of a 100-fold excess of unlabeled JMV4168 or JMV5132. Small-animal PET/CT clearly visualized PC-3 tumors, with the highest resolution observed for Al[18]F-JMV5132. **Conclusion:** JMV5132 could be rapidly and efficiently labeled with [18]F. Al[18]F-JMV5132, ^{68}Ga-JMV5132, and ^{68}Ga-JMV4168 all showed comparable high and specific accumulation in GRPR-positive PC-3 tumors. These new PET tracers are promising candidates for future clinical translation.

Key Words: GRPR; bombesin; PET; ^{18}F; prostate cancer

Prostate cancer (PCa) is the most frequently diagnosed cancer and the second leading cause of cancer death among men in the United States (*1*). There is a strong need for improved imaging techniques that provide accurate staging and monitoring of this disease, particularly at early stages. Conventional diagnostic techniques, such as ultrasound-guided biopsy, are limited by high false-negative rates (*2*). Emerging functional imaging techniques, including diffusion-weighted MR imaging, dynamic contrast-enhanced MR imaging, and PET, have shown improved sensitivity and staging accuracy for detecting primary prostate tumors and metastatic lymph nodes (*3*). Several PET radiotracers have shown promising clinical utility, such as the metabolic agents ^{18}F-FDG, [11]C-/^{18}F-choline, and [11]C-/^{18}F-acetate for the assessment of distant metastasis and ^{18}F-NaF for the detection of bone metastasis (*4*). However, their application is most valuable in late-stage, recurrent, or metastatic PCa. Increasing efforts are being made in developing PET imaging agents targeting specific biomarkers of PCa, such as gastrin-releasing peptide receptor (GRPR) (*5*) and prostate-specific membrane antigen (*6*).

The GRPR, or bombesin (BBN) receptor subtype II, has been shown to be overexpressed in several human tumors, including PCa (*7*). Overexpression of GRPR was found in 63%–100% of primary prostate tumors and more than 50% of lymph and bone metastases (*8,9*). The GRPR density was reported to be 26-fold higher in prostate carcinoma than prostatic hyperplasia (*9*). Because of the low expression in benign prostatic hyperplasia and inflammatory prostatic tissues, imaging of GRPR in localized PCa has potential advantages over choline- and acetate-based radiotracers (*9,10*).

A variety of radiolabeled BBN analogs have been developed for targeting GRPR-positive tumors and were evaluated in preclinical

and clinical studies (5). Several recent reports have shown that GRPR antagonists show properties superior to GRPR agonists, affording higher tumor uptake and lower accumulation in physiologic GRPR-positive nontarget tissues (11,12). Moreover, GRPR agonists were shown to induce side effects in patients, mediated by virtue of their physiologic activity (13,14). Therefore, particular attention has been drawn to the development of GRPR antagonists for imaging and radionuclide therapy of PCa. Several GRPR antagonists have since been developed by the modification of C-terminal residues of GRPR agonists, including the statin-based BBN analog, JMV594 (H-D-Phe-Gln-Trp-Ala-Val-Gly-His-Sta-Leu-NH$_2$) (15).

^{68}Ga-labeled GRPR antagonists were developed for PET imaging, showing good targeting properties in preclinical studies (12,16–18) and recently also in clinical trials (19,20). Clinical evaluation of the ^{68}Ga-labeled GRPR antagonist BAY86-7548 (^{68}Ga-DOTA-4-amino-1-carboxymethylpiperidine-D-Phe-Gln-Trp-Ala-Val-Gly-His-Sta-Leu-NH$_2$) has shown a specificity, sensitivity, and accuracy of 88%, 81%, and 83%, respectively, for the detection of primary PCa. In comparison, it was shown that ^{11}C-choline was not able to discriminate PCa from benign prostatic hyperplasia, because maximum standardized uptake values in PCa were not significantly different from benign prostatic hyperplasia (21). Another study reported a specificity, sensitivity, and accuracy of 80%, 29%, and 71%, respectively, for the detection of PCa using ^{11}C-choline (22). The detection of lymph node metastases with the ^{68}Ga-labeled GRPR antagonist was suboptimal, partially due to the suboptimal physical characteristics of ^{68}Ga, limiting the detection of small lesions (20). Therefore, the aim of the present study was to develop an ^{18}F-labeled GRPR antagonist for high-resolution and sensitive PET imaging of primary, recurrent, and metastatic PCa and to compare the imaging properties of this tracer with those of ^{68}Ga-labeled analogs. ^{18}F has superior physical characteristics for PET imaging, such as a lower positron range and a higher positron yield, offering higher resolution and sensitivity (23). However, most methods for labeling peptides with ^{18}F are laborious and require multistep procedures with moderate labeling yields. A good alternative is the Al^{18}F-labeling method (24), allowing fast and facile labeling of peptides in a 1-step procedure. We designed a new GRPR antagonist conjugate (JMV5132 [NODA-MPAA-βAla-βAla-(H-D-Phe-Gln-Trp-Ala-Val-Gly-His-Sta-Leu-NH$_2$); NODA-MPAA is 2-(4-(carboxymethyl)-7-{[4-(carboxymethyl)phenyl]methyl}-1,4,7-triazacyclononan-1-yl)acetic acid]),

analogous to the previously described JMV4168 (DOTA-βAla-βAla-[H-D-Phe-Gln-Trp-Ala-Val-Gly-His-Sta-Leu-NH$_2$]) (25), with a NODA-MPAA chelator for high-yield complexation of Al^{18}F (26). Here, we report on the direct preclinical comparison of 3 novel radiolabeled tracers (Al^{18}F-JMV5132, ^{68}Ga-JMV4168, and ^{68}Ga-JMV5132) for PET imaging of PCa. We determined the in vitro characteristics of the radiolabeled peptides and evaluated their tumor targeting properties in vivo in nude mice with subcutaneous human prostate tumors.

MATERIALS AND METHODS

Synthesis of JMV4168 and JMV5132

JMV4168 was synthesized using Fmoc-based solid-phase peptide synthesis as described previously (25). JMV5132 was synthesized in the same manner as JMV4168 but was coupled to tert-butyl (tBu)–protected NODA-MPAA instead of tBu-protected DOTA. NODA-MPAA was prepared as previously described using NO2AtBu (Chematech) (26). The chemical structures of JMV4168 and JMV5132 are shown in Figure 1.

Radiolabeling

Radiolabeling of JMV5132 with Al^{18}F. ^{18}F$^-$ solution in enriched water (BV Cyclotron, VU) was purified from metal impurities and concentrated before use, as described in the supplemental materials (available at http://jnm.snmjournals.org). Labeling was performed by mixing ^{18}F$^-$ solution (15–20 μL, 700–900 MBq), sodium acetate (NaOAc) (0.5 μL of 1 M solution, pH 4.1), Al^{3+} stock solution (20 nmol, 10 μL of 2 mM AlCl$_3$·6H$_2$O in 0.1 M NaOAc, pH 4.2), acetonitrile (67% v/v), quenchers (2.5 μL of 50 mM methionine, gentisic acid, and ascorbic acid), and finally JMV5132 (20 nmol, 3.26 μL of solution [10 μg/μL] in 2 mM NaOAc, pH 4.1). The reaction mixture was heated for 15 min at 105°C. To allow injection into mice, the peptide was diluted to less than 0.5% (v/v) acetonitrile with 0.5% (w/v) bovine serum albumin, 0.5% (w/v) polyoxyethylene (20) sorbitan monolaurate solution (polysorbate-20), and quenchers (1 mM methionine, gentisic acid, and ascorbic acid) in phosphate-buffered saline (PBS), pH 7.4. Bovine serum albumin and polysorbate-20 were added to reduce binding of radiolabeled peptide to plastic disposables, whereas quenchers (methionine, gentisic acid, and ascorbic acid) were added to prevent radiolysis of radiolabeled peptides.

Radiolabeling of JMV4168 and JMV5132 with ^{68}Ga. Elution and purification of ^{68}Ga from a ^{68}Ga/^{68}Ge generator (IGG-100; Eckert & Ziegler Europe) was performed using the sodium chloride–based procedure described earlier (27). A volume of 375 μL of 4-(2-hydroxyethyl)piperazine-1-ethanesulfonic acid (1 M, pH 3.6) was slowly added to 300 μL of purified ^{68}Ga eluate, followed by addition of quenchers (methionine, gentisic acid, and ascorbic acid, 1.25 mM) and peptide (2 nmol). The reaction mixture was heated for 10 min at 95°C. After reaction, ethylenediaminetetraacetic acid (50 mM) was added to a final concentration of 5 mM to complex free ^{68}Ga. For animal experiments, the labeled product was purified by reversed-phase high-performance liquid chromatography (RP-HPLC) using the gradient described in the "Quality Control" section of the supplemental materials and concentrated by evaporation. To allow injection into mice, the radiolabeled peptide was diluted with 0.5% (w/v) bovine serum albumin, 0.5% (w/v) polysorbate-20, and quenchers (1 mM methionine, gentisic acid, and ascorbic acid) in PBS and neutralized with sodium carbonate (NaHCO$_3$) buffer (1 M, pH 8.5).
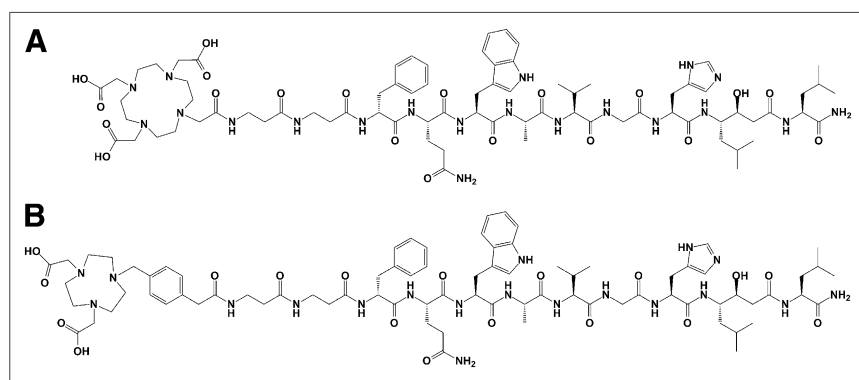

FIGURE 1. Chemical structures of DOTA-βAla-βAla-[H-D-Phe-Gln-Trp-Ala-Val-Gly-His-Sta-Leu-NH$_2$] (JMV4168) (A) and NODA-MPAA-βAla-βAla-[H-D-Phe-Gln-Trp-Ala-Val-Gly-His-Sta-Leu-NH$_2$] (JMV5132) (B).
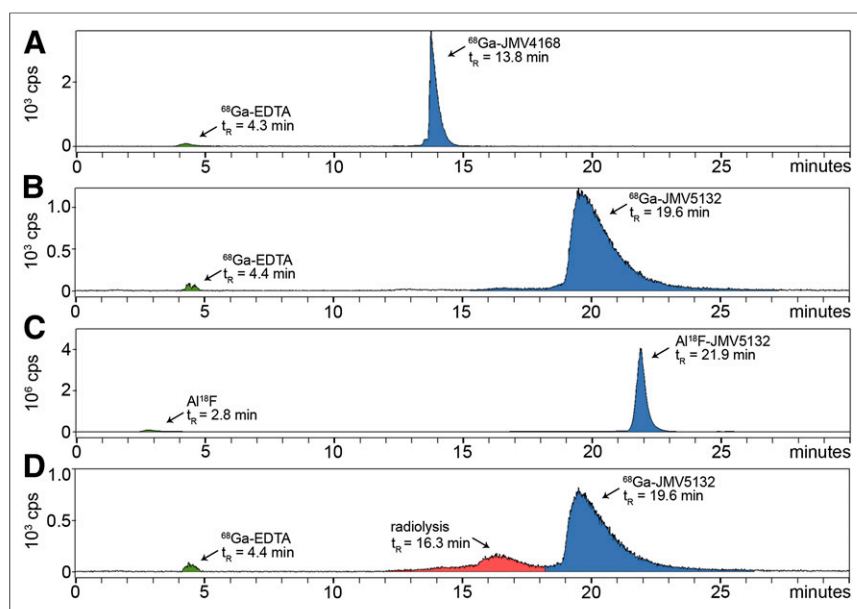
FIGURE 2. Radio–high-performance liquid chromatograms of ^{68}Ga-JMV4168 (A), ^{68}Ga-JMV5132 (B), and Al^{18}F-JMV5132 (C). (D) Radio–high-performance liquid chromatogram of ^{68}Ga-JMV5132 without added quenchers. y-axis = radioactivity in count per second (cps); x-axis = retention time in min. EDTA = ethylenediaminetetraacetic acid; t_R = retention time.

Cold Labeling of JMV4168 and JMV5132 with ^{nat}Ga and ^{nat}F. The labeling methods of JMV4168 and JMV5132 with ^{nat}Ga and ^{nat}F are described in the supplemental materials.

Quality Control

Quality control methods for peptide synthesis and radiolabeling are described in detail in the supplemental materials.

Lipophilicity. The octanol/PBS partition coefficients of ^{68}Ga-JMV4168, ^{68}Ga-JMV5132, and Al^{18}F-JMV5132 were determined as described previously (28).

Cell Culture and Competitive Cell Binding Assay

The human PCa cell line PC-3 was cultured in Ham F-12K (Kaighn's) medium (Life Technologies) supplemented with 10% fetal calf serum, penicillin (100 units/mL), and streptomycin (100 μg/mL). Cells were grown in tissue culture flasks at 37°C in a humidified atmosphere containing 5% CO_2.

The binding affinities of JMV4168, JMV5132, ^{nat}Ga-JMV4168, ^{nat}Ga-JMV5132, and Al^{nat}F-JMV5132 toward the GRPR were determined in a competitive binding assay using frozen cryostat sections (10-μm thick) of PC-3 xenografts and [^{125}I-Tyr^4]-BBN as a tracer. Tyr^4-BBN (Sigma Aldrich) was iodinated as described earlier (29). The competitive binding assay protocol is described in detail in the supplemental materials.

Small-Animal PET/CT and Biodistribution Studies

Male nude BALB/c mice (age, 6–8 wk) were injected subcutaneously near the right shoulder with a PC-3 cell suspension (5×10^6 cells, 200 μL, 66% RPMI, 33% Matrigel [BD Biosciences]). Two to 3 wk after inoculation, when tumor size averaged 200 mm^3, mice were injected intravenously with 5–10 MBq of radiolabeled peptide (200 pmol, 200 μL). To confirm the receptor specificity of the radiolabeled peptides, additional animals were coinjected with an excess (20 nmol) of unlabeled peptide. Mice were euthanized 1 or 2 h after injection by CO_2/O_2 asphyxiation. Mice were first scanned prone on a small-animal PET/CT scanner (Inveon; Siemens Preclinical Solutions). PET emission scans

were acquired for 30–60 min, followed by a CT scan. After scanning, blood, tumor, and relevant organs and tissues were collected, weighed, and counted in a γ counter. Scanning and reconstruction parameters, as well as counting parameters, are described in detail in the supplemental materials. The percentage injected dose per gram (%ID/g) was determined for each tissue sample. All animal experiments were approved by local authorities and were in compliance with the institutions guidelines.

Statistical Analysis

Statistical analysis was performed using GraphPad Prism (version 5.01; GraphPad Software) and described in the supplemental materials.

RESULTS

Synthesis of JMV4168 and JMV5132

JMV4168 and JMV5132 (Fig. 1) were obtained with an average yield of approximately 40% and a purity greater than 97% as confirmed by RP-HPLC. Conjugates were characterized by electrospray ionization mass spectroscopy (mass/charge, [M+2H]$^{2+}$/2: JMV4168, calculated: 815.9414, found: 815.9412; JMV5132, calculated: 821.4416, found: 821.4433).

Radiolabeling and Stability Studies

Al^{18}F-JMV5132 was obtained with a specific activity of 40 ± 4 MBq/nmol (88% non–decay-corrected yield) and ^{68}Ga-JMV4168 and ^{68}Ga-JMV5132 with a specific activity of 47 ± 2 and 47 ± 4 MBq/nmol after purification, respectively. RP-HPLC analysis indicated that the radiochemical purity of the Al^{18}F- or ^{68}Ga-labeled peptide preparations used in in vitro and in vivo experiments always exceeded 95%. Radio-HPLC elution profiles of Al^{18}F- and ^{68}Ga-labeled peptides are shown in Figure 2A. ^{68}Ga-JMV4168, ^{68}Ga-JMV5132, and Al^{18}F-JMV5132 had retention times of 13.8, 19.6, and 21.9 min, respectively. The addition of quenchers (methionine, gentisic acid, and ascorbic acid) prevented oxidation of the radiolabeled peptides, as shown in Figure 2B.

Lipophilicity

The octanol/PBS partition coefficients were determined to estimate the lipophilicity of the Al^{18}F- or ^{68}Ga-labeled peptides. The log $P_{octanol/PBS}$ values for ^{68}Ga-JMV4168, ^{68}Ga-JMV5132, and Al^{18}F-JMV5132 were −2.53 ± 0.04, −1.40 ± 0.01, and −1.56 ± 0.08, respectively. This result shows that the ^{68}Ga-DOTA analog (JMV4168) was more hydrophilic than the ^{68}Ga- and ^{18}F-NODA-MPAA analogs (JMV5132).

Competitive Cell Binding Assay

The affinity of JMV4168, JMV5132, ^{nat}Ga-JMV4168, ^{nat}Ga-JMV5132, and Al^{nat}F-JMV5132 for the GRPR was determined in a competitive binding assay, using [^{125}I-Tyr^4]-BBN as radioligand. The displacement binding curves are shown in Figure 3. Inhibitory concentration of 50% (IC$_{50}$) values (in nM) for binding to GRPR for JMV5132 (NODA-MPAA), JMV4168 (DOTA), and Al^{nat}F-JMV5132 were not significantly different: 6.8 (95%
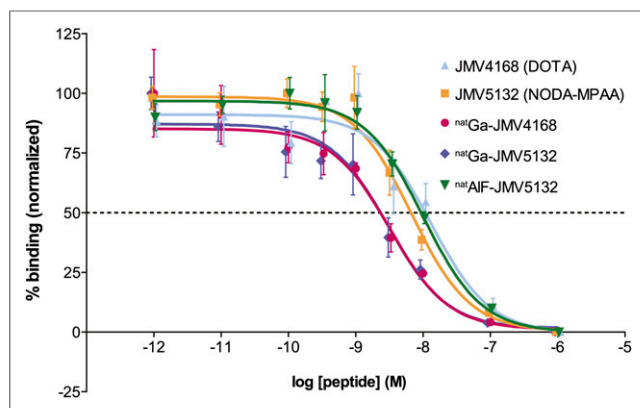
FIGURE 3. Competition binding curves. PC-3 frozen sections were incubated in presence of 5.10^{-10} M [^{125}I-Tyr^4]-BBN and increasing amounts of JMV4168, JMV5132, ^{nat}Ga-JMV4168, or ^{nat}Ga-JMV5132. IC_{50} values (with 95% CIs in parentheses) were 6.8 nM (4.6–10.0) for JMV5132, 13.2 nM (5.9–29.3) for JMV4168, 3.0 nM (1.5–6.0) for ^{nat}Ga-JMV5132, 3.2 nM (1.8–5.9) for ^{nat}Ga-JMV4168, and 10.0 nM (6.3–16.0) for Al^{nat}F-JMV5132.

confidence interval [CI], 4.6–10.0), 13.2 (95% CI, 5.9–29.3), and 10.0 nM (95% CI, 6.3–16.0), respectively. IC_{50} values for ^{nat}Ga-JMV5132 (3.0 [95% CI, 1.5–6.0]) and ^{nat}Ga-JMV4168 (3.2 [95% CI, 1.8–5.9]) were lower than their unlabeled counterpart, indicating a higher binding affinity for the GRPR.

Small-Animal PET/CT and Biodistribution Studies

Fused PET and CT images obtained at 1 and 2 h after injection are shown in Figure 4. Maximum-intensity projections showed clear visualization of PC-3 tumors with very low background. Predominant renal excretion was observed for all 3 radiolabeled peptides. Partial hepatobiliary excretion was observed for Al^{18}F-JMV5132 and ^{68}Ga-JMV5132, as indicated by the nonspecific uptake in the gallbladder and intestines. PET images obtained at 2 h after injection showed partial clearance of radioactivity in nontarget tissues such as pancreas, kidney, and intestines as compared with the images obtained at 1 h after injection.

The results of the biodistribution studies of ^{18}F- and ^{68}Ga-labeled peptides are summarized in Figure 5. These pharmacokinetic data obtained at 1 and 2 h after injection were in line with the PET images. High and specific uptake of the tracer was observed in the PC-3 tumors. There were no significant differences for ^{68}Ga-JMV4168, ^{68}Ga-JMV5132, and Al^{18}F-JMV5132, with uptake values (in %ID/g) of 4.46 ± 0.33, 4.73 ± 0.68, and 4.96 ± 1.20, respectively, at 1 h after injection and 5.96 ± 1.39, 5.24 ± 0.29, and 5.30 ± 0.98, respectively, at 2 h after injection. The uptake in GRPR-positive organs, such as tumor, pancreas, stomach, and intestines, was significantly decreased by coinjection of an excess of unlabeled peptide, indicating GRPR-specific targeting. All tracers displayed fast blood clearance, with 0.09 ± 0.04, 0.19 ± 0.13, and 0.05 ± 0.01 %ID/g remaining in blood at 2 h after injection for ^{68}Ga-JMV4168, ^{68}Ga-JMV5132, and Al^{18}F-JMV5132, respectively. The 3 tracers cleared rapidly from the GRPR-positive pancreas between 1 h (6.14 ± 0.68, 11.42 ± 0.84, and 4.21 ± 1.34 %ID/g) and 2 h after injection (1.00 ± 0.24, 1.33 ± 0.25, and 1.41 ± 0.15 %ID/g) for ^{68}Ga-JMV4168, ^{68}Ga-JMV5132, and Al^{18}F-JMV5132, respectively, whereas PC-3 tumor uptake was preserved. The uptake and retention of all tracers in blood, muscle,
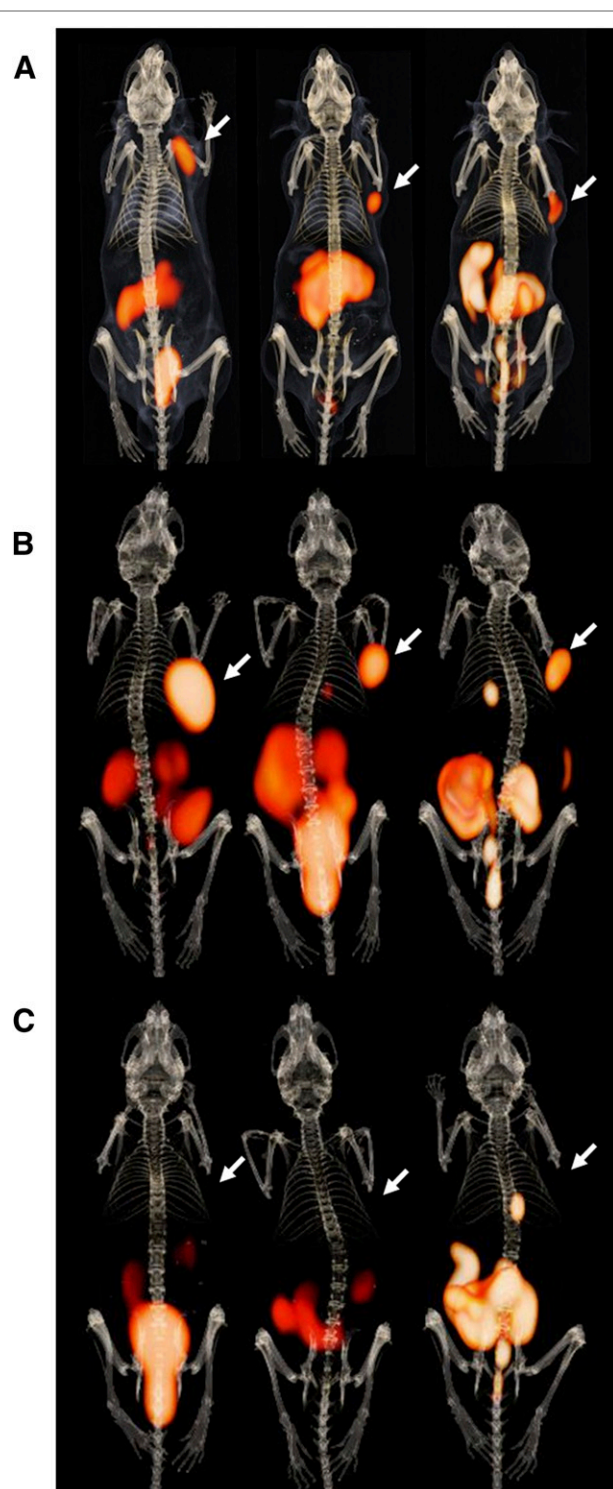

FIGURE 4. PET/CT images of mice bearing subcutaneous PC-3 xenografts on right shoulder (arrow) injected with ^{68}Ga-JMV4168 (left), ^{68}Ga-JMV5132 (center), or Al^{18}F-JMV5132 (right) at 1 h after injection (A), 2 h after injection (B), and 2 h after injection with coinjection of excess unlabeled peptide (C). Besides tumor (arrow), pancreas, intestines, and kidneys can be observed in abdominal region. Bladder can be distinguished by hot spot below abdomen. Gallbladder can be recognized as hot spot below rib cage.
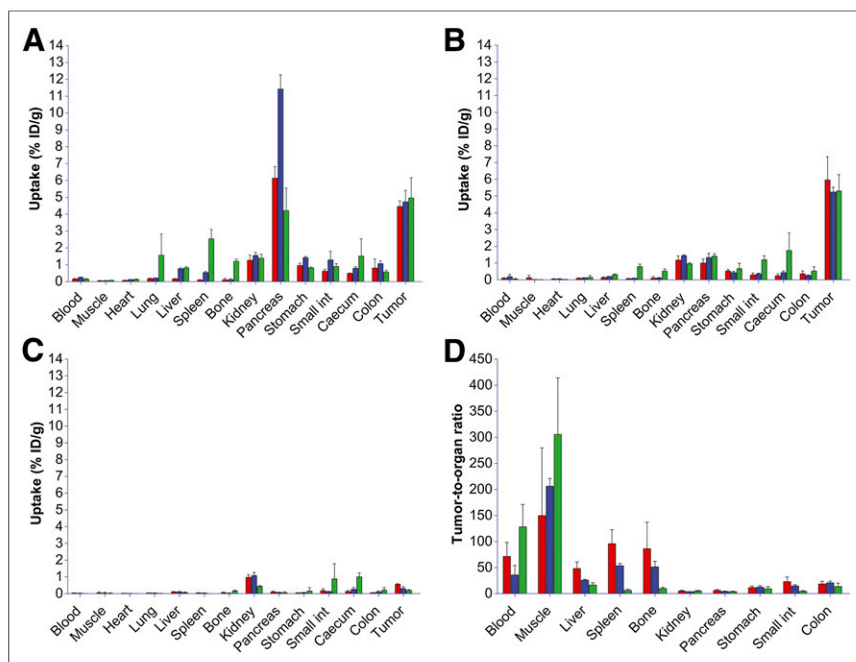
FIGURE 5. Biodistribution of ^{68}Ga-JMV4168 (red), ^{68}Ga-JMV5132 (blue), and Al[18]F-JMV5132 (green) in mice bearing PC-3 xenografts at 1 h after injection (A), 2 h after injection (B), and 2 h after injection with coinjection of excess unlabeled peptide (C) and tumor-to-organ ratios at 2 h after injection (D). Int = intestines.

heart, lung, liver, and bone were relatively low as measured at 2 h after injection (all ≤0.5 %ID/g). Mice injected with Al[18]F-JMV5132 showed a (significantly) higher uptake in spleen and bone.

DISCUSSION

The use of radiolabeled GRPR antagonists for targeting tumors in vivo has attracted considerable attention, starting with somatostatin receptor antagonists showing higher tumor uptake and targeting more receptor-binding sites than their agonists (30). This finding was also extended to GRPR antagonists, with the seminal work of Cescato et al. (11). Recently, more articles have appeared showing the promise of novel radiolabeled GRPR antagonists for GRPR-positive tumor imaging (12,16–18,25). The studies revealed favorable pharmacokinetics of radiolabeled antagonists, including high tumor uptake and fast clearance from nontargeted tissues. Several [64]Cu- and ^{68}Ga-labeled receptor antagonists developed for PET imaging of prostate tumors have shown pharmacokinetics superior to [64]Cu- or ^{18}F-labeled GRPR agonists described in earlier literature (12,16,17). Besides a favorable pharmacokinetic profile, the use of antagonists should reduce the occurrence of side effects. In a study in which BBN was infused intravenously in a dose of 15 ng/kg/min over a 90-min period, side effects—among which were nausea, hot flush, and sweating—were observed in 80% of the patients (13).

Here, we report on the development of a NODA-MPAA–conjugated GRPR antagonist (JMV5132) labeled with ^{18}F for PET imaging of GRPR-positive tumors and the direct comparison with ^{68}Ga-radiolabeled analogs. In our previous work, the statin-based GRPR antagonist JMV594 was linked to DOTA via a (βAla)2 linker and labeled with [111]In. It showed good tumor targeting in PC-3

xenografts in mice (25). In the present study, we conjugated JMV594 to NODA-MPAA for radiolabeling with [18]F. The NODA-MPAA-(βAla)2-JMV594 peptide (JMV5132) was labeled with ^{18}F and ^{68}Ga and compared with the ^{68}Ga-labeled DOTA-(βAla)2-JMV594 peptide (JMV4168).

The radiolabeling of peptides via complexation of Al[18]F by a NOTA chelator was first described by McBride et al. (24). This novel technique has been successfully applied to several peptides, including a GRPR agonist (28) and recently to GRPR antagonists (31,32). Recently, McBride et al. reported the labeling of peptides with Al[18]F in a 1-pot, 1-step procedure using the NODA-MPAA chelator (26, 33), leading to a kit formulation, after which the labeled peptide could be purified by solid-phase extraction.

In the present study, we further optimized the labeling conditions to achieve Al[18]F-labeled JMV5132 in less than 20 min with complete incorporation of ^{18}F-fluoride, resulting in a high specific activity (35 MBq/nmol), without the need for purification by solid-phase extraction. In receptor-binding studies using PC-3 tumor sections, the in vitro affinities of JMV5132 and JMV4168 were comparable, as shown by the similar IC_{50} values, indicating that both chelators apparently affected receptor affinity in a similar way. The peptides labeled with [nat]Ga had slightly higher receptor affinities than their unlabeled counterpart, indicating that the presence of Ga^{3+} in the chelator enhanced the affinity of the peptides for the GRPR. The affinity of the peptide labeled with [nat]AlF, on the other hand, was not significantly different from its unlabeled counterpart, indicating that the presence of AlF in the chelator did not affect the affinity of the peptide for the GRPR.

The PET images obtained with Al[18]F-JMV5132 showed higher spatial resolution than the images obtained with the ^{68}Ga-labeled tracers, which is most likely due to the longer positron range of [68]Ga (34) as compared with [18]F.

The comparative biodistribution study showed GRPR-specific accumulation of all 3 radiolabeled GRPR antagonists in the tumor. ^{68}Ga-JMV4168, ^{68}Ga-JMV5132, and Al[18]F-JMV5132 tracers showed similar uptake in the GRPR-positive tumor and organs, including PC-3 tumor, pancreas, stomach, and colon. The uptake was receptor-mediated, as confirmed by the reduction of uptake in tumor and other receptor-positive organs after coinjection of excess unlabeled peptide. The washout from receptor-positive organs occurred at different rates. The pancreas uptake decreased from 1 to 2 h after injection by a factor of 6.1, 8.6, and 3.0 for ^{68}Ga-JMV4168, ^{68}Ga-JMV5132, and Al[18]F-JMV5132, respectively, whereas tumor uptake was increased by a factor of 1.3, 1.1, and 1.1 for ^{68}Ga-JMV4168, ^{68}Ga-JMV5132, and Al[18]F-JMV5132, respectively. This outcome indicates a higher retention of the tracers in the tumor than in the pancreas.

Despite their low internalization rate, the high and persistent tumor uptake of these radiolabeled antagonists was expected, as it was previously described for a few other radiolabeled

antagonists (*11,12,16,18*). This might be explained by a higher number of binding sites for receptor antagonists than agonists, a higher metabolic stability of antagonists, or a strong interaction of the antagonist with the receptor (*11,16*). In previous studies using radiolabeled GRPR antagonists, a faster clearance from the pancreas and abdominal organs was already observed between 1 and 4 h after injection, in contrast with data concerning radiolabeled GRPR agonists, which showed more sustained retention of activity in the abdominal region. Several reasons for these differences in tissue clearance kinetics have been postulated, including species differences or more efficient perfusion in the pancreas and intestine (*16*). Possible metabolic degradation of the peptide by enzymes in the pancreas might also explain the faster washout from the pancreas.

Clearance from background tissues, such as blood, muscle, heart, lung, liver, and bone, was fast for all tracers tested, leading to high tumor-to-background ratios, which allowed clear visualization of the tumor. Overall, Al^{18}F-JMV5132 showed improved imaging properties, compared with the previously reported Al^{18}F-NOTA-8-Aoc-BBN(7-14)NH$_2$ GRPR agonist (*28*), because that analog showed lower tumor uptake, much higher pancreatic uptake, and higher liver and intestinal uptake in the same animal model.

The slightly higher uptake of Al^{18}F-JMV5132 in bone may be due to the presence of trace amounts (<1%) of uncomplexed Al^{18}F or ^{18}F-fluoride or partial defluorination of the tracer in vivo. The uptake of Al^{18}F-JMV5132 in bone was relatively low (0.52 ± 0.13 %ID/g 2 h after injection), in comparison with the values reported for the Al^{18}F-labeled RM1 derivative (1.58 %ID/g 2 h after injection) (*31*). The increased uptake of Al^{18}F-JMV5132 and ^{68}Ga-JMV5132 in the gallbladder, liver, and gastrointestinal excretions indicates partial hepatobiliary excretion of the tracers, because of their higher lipophilicity, which may be caused by the benzyl group. Considering the clinical application of the tracers, high signal intensity in the intestines may affect visualization of prostate-confined tumor or spread to lymph nodes. Nevertheless, considering the superior imaging characteristics of ^{18}F, further development of Al^{18}F-JMV5132 as a tracer for PCa diagnostic and therapy follow-up is certainly warranted.

CONCLUSION

Highly sensitive and receptor-specific imaging of PCa with PET/CT can be achieved using ^{68}Ga- and ^{18}F-labeled GRPR antagonists. In this study, labeling of JMV5132 with Al^{18}F was completed within 20 min with high specific activity without a need for purification. The ^{68}Ga-JMV4168 tracer showed the most favorable biodistribution, because of its lower hepatobiliary excretion, but the PET images showed a higher resolution with the ^{18}F-JMV5132 tracer. These new PET tracers are promising candidates for future clinical translation.

DISCLOSURE

ACKNOWLEDGMENTS

REFERENCES

1. Siegel R, Naishadham D, Jemal A. Cancer statistics, 2012. *CA Cancer J Clin.* 2012;62:10–29.
2. Roehl KA, Antenor JA, Catalona WJ. Serial biopsy results in prostate cancer screening study. *J Urol.* 2002;167:2435–2439.
3. Talab SS, Preston MA, Elmi A, Tabatabaei S. Prostate cancer imaging: what the urologist wants to know. *Radiol Clin North Am.* 2012;50:1015–1041.
4. Mari Aparici C, Seo Y. Functional imaging for prostate cancer: therapeutic implications. *Semin Nucl Med.* 2012;42:328–342.
5. Sancho V, Di Florio A, Moody TW, Jensen RT. Bombesin receptor-mediated imaging and cytotoxicity: review and current status. *Curr Drug Deliv.* 2011;8:79–134.
6. Osborne JR, Akhtar NH, Vallabhajosula S, Anand A, Deh K, Tagawa ST. Prostate-specific membrane antigen-based imaging. *Urol Oncol.* 2013;31:144–154.
7. Reubi JC, Wenger S, Schmuckli-Maurer J, Schaer JC, Gugger M. Bombesin receptor subtypes in human cancers: detection with the universal radioligand ^{125}I-[D-TYR^6, β-ALA^{11}, PHE^{13}, NLE^{14}] bombesin(6-14). *Clin Cancer Res.* 2002;8:1139–1146.
8. Ananias HJ, van den Heuvel MC, Helfrich W, de Jong IJ. Expression of the gastrin-releasing peptide receptor, the prostate stem cell antigen and the prostate-specific membrane antigen in lymph node and bone metastases of prostate cancer. *Prostate.* 2009;69:1101–1108.
9. Markwalder R, Reubi JC. Gastrin-releasing peptide receptors in the human prostate: relation to neoplastic transformation. *Cancer Res.* 1999;59:1152–1159.
10. Beer M, Montani M, Gerhardt J, et al. Profiling gastrin-releasing peptide receptor in prostate tissues: clinical implications and molecular correlates. *Prostate.* 2012;72:318–325.
11. Cescato R, Maina T, Nock B, et al. Bombesin receptor antagonists may be preferable to agonists for tumor targeting. *J Nucl Med.* 2008;49:318–326.
12. Mansi R, Wang X, Forrer F, et al. Evaluation of a 1,4,7,10-tetraazacyclododecane-1,4,7,10-tetraacetic acid-conjugated bombesin-based radioantagonist for the labeling with single-photon emission computed tomography, positron emission tomography, and therapeutic radionuclides. *Clin Cancer Res.* 2009;15:5240–5249.
13. Basso N, Lezoche E, Speranza V. Studies with bombesin in man. *World J Surg.* 1979;3:579–585.
14. Bodei L, Ferrari M, Nunn A, et al. ^{177}Lu-AMBA bombesin analogue in hormone refractory prostate cancer patients: a phase I escalation study with single-cycle administrations. *Eur J Nucl Med Mol Imaging.* 2007;34:S221.
15. Llinares M, Devin C, Chaloin O, et al. Syntheses and biological activities of potent bombesin receptor antagonists. *J Pept Res.* 1999;53:275–283.
16. Mansi R, Wang X, Forrer F, et al. Development of a potent DOTA-conjugated bombesin antagonist for targeting GRPr-positive tumours. *Eur J Nucl Med Mol Imaging.* 2011;38:97–107.
17. Abiraj K, Mansi R, Tamma ML, et al. Bombesin antagonist-based radioligands for translational nuclear imaging of gastrin-releasing peptide receptor-positive tumors. *J Nucl Med.* 2011;52:1970–1978.
18. Varasteh Z, Velikyan I, Lindeberg G, et al. Synthesis and characterization of a high-affinity NOTA-conjugated bombesin antagonist for GRPR-targeted tumor imaging. *Bioconjug Chem.* 2013;24:1144–1153.
19. Roivainen A, Kahkonen E, Luoto P, et al. Plasma pharmacokinetics, whole-body distribution, metabolism, and radiation dosimetry of ^{68}Ga bombesin antagonist BAY 86-7548 in healthy men. *J Nucl Med.* 2013;54:867-872.
20. Kahkonen E, Jambor I, Kemppainen J, et al. In vivo imaging of prostate cancer using [^{68}Ga]-labeled bombesin analog BAY86-7548. *Clin Cancer Res.* 2013;19:5434–5443.

21. Souvatzoglou M, Weirich G, Schwarzenboeck S, et al. The sensitivity of [11C] choline PET/CT to localize prostate cancer depends on the tumor configuration. *Clin Cancer Res.* 2011;17:3751–3759.

22. Jambor I, Borra R, Kemppainen J, et al. Functional imaging of localized prostate cancer aggressiveness using 11C-acetate PET/CT and 1H-MR spectroscopy. *J Nucl Med.* 2010;51:1676–1683.

23. Sanchez-Crespo A. Comparison of gallium-68 and fluorine-18 imaging characteristics in positron emission tomography. *Appl Radiat Isot.* 2013;76:55–62.

24. McBride WJ, Sharkey RM, Karacay H, et al. A novel method of 18F radiolabeling for PET. *J Nucl Med.* 2009;50:991–998.

25. Marsouvanidis PJ, Nock BA, Hajjaj B, et al. Gastrin releasing peptide receptor-directed radioligands based on a bombesin antagonist: synthesis, 111In-labeling, and preclinical profile. *J Med Chem.* 2013;56:2374–2384.

26. D'Souza CA, McBride WJ, Sharkey RM, Todaro LJ, Goldenberg DM. High-yielding aqueous 18F-labeling of peptides via Al18F chelation. *Bioconjug Chem.* 2011;22:1793–1803.

27. Mueller D, Klette I, Baum RP, Gottschaldt M, Schultz MK, Breeman WA. Simplified NaCl based 68Ga concentration and labeling procedure for rapid synthesis of 68Ga radiopharmaceuticals in high radiochemical purity. *Bioconjug Chem.* 2012;23:1712–1717.

28. Dijkgraaf I, Franssen GM, McBride WJ, et al. PET of tumors expressing gastrin-releasing peptide receptor with an 18F-labeled bombesin analog. *J Nucl Med.* 2012;53:947–952.

29. de Blois E, Chan HS, Breeman WA. Iodination and stability of somatostatin analogues: comparison of iodination techniques: a practical overview. *Curr Top Med Chem.* 2012;12:2668–2676.

30. Ginj M, Zhang H, Waser B, et al. Radiolabeled somatostatin receptor antagonists are preferable to agonists for in vivo peptide receptor targeting of tumors. *Proc Natl Acad Sci USA.* 2006;103:16436–16441.

31. Liu Y, Hu X, Liu H, et al. A comparative study of radiolabeled bombesin analogs for the PET imaging of prostate cancer. *J Nucl Med.* 2013;54:2132–2138.

32. Varasteh Z, Aberg O, Velikyan I, et al. In vitro and in vivo evaluation of a 18F-labeled high affinity nota conjugated bombesin antagonist as a PET ligand for GRPR-targeted tumor imaging. *PLoS ONE.* 2013;8:e81932.

33. McBride WJ, D'Souza CA, Karacay H, Sharkey RM, Goldenberg DM. New lyophilized kit for rapid radiofluorination of peptides. *Bioconjug Chem.* 2012;23:538–547.

34. Disselhorst JA, Brom M, Laverman P, et al. Image-quality assessment for several positron emitters using the NEMA NU 4-2008 standards in the Siemens Inveon small-animal PET scanner. *J Nucl Med.* 2010;51:610–617.

The Journal of NUCLEAR MEDICINE

Preclinical Comparison of Al^{18}F- and ^{68}Ga-Labeled Gastrin-Releasing Peptide Receptor Antagonists for PET Imaging of Prostate Cancer

Kristell L.S. Chatalic, Gerben M. Franssen, Wytske M. van Weerden, William J. McBride, Peter Laverman, Erik de Blois, Bouchra Hajjaj, Luc Brunel, David M. Goldenberg, Jean-Alain Fehrentz, Jean Martinez, Otto C. Boerman and Marion de Jong

This article and updated information are available at:
http://jnm.snmjournals.org/content/55/12/2050

Information about reproducing figures, tables, or other portions of this article can be found online at:
http://jnm.snmjournals.org/site/misc/permission.xhtml

Information about subscriptions to JNM can be found at:
http://jnm.snmjournals.org/site/subscriptions/online.xhtml

SNMMI | SOCIETY OF NUCLEAR MEDICINE AND MOLECULAR IMAGING